buildings

MDPI

Article

Diffusion Characteristics of PM2.5 in Rural Dwelling under Different Daily Life Behavior: A Case Study in Rural Shenyang of China

Xueyan Zhang [1,*], Yiming Yang [1], Guanhua Huang [1], Bin Chen [1], Yu Chen [2], Joe R. Zhao [3] and Helen J. Sun [3]

[1] School of Civil Engineering, Dalian University of Technology, Dalian 116024, China
[2] School of Hydraulic and Civil Engineering, Zhengzhou University, Zhengzhou 450000, China
[3] Tri-Y Environmental Research Institute, 2655 Lillooet St., Vancouver, BC V5M 4P7, Canada
* Correspondence: xueyan@dlut.edu.cn; Tel.: +86-15842425608

Abstract: The highest concentration of PM2.5 in cold rural dwellings of Northeast China is often generated by using mini stoves for cooking and heating, which can directly influence human health. As of yet, little is known about the impact of different daily life behavior on PM2.5 diffusion and residents' exposure in rural dwellings. In this study, the characteristics of indoor PM2.5 variation and diffusion in rural dwellings was described by measuring some rural dwellings and establishing a multi-zone network model. The calculated results indicated that the relative errors between theoretical calculated results and experimental measured results are within 10%. PM2.5 diffusion in a rural dwelling can be predicted. Furthermore, the impacts of daily life behavior on PM2.5 diffusion and exposure assessment can be analyzed. Through discussion, heating behavior is the most important factor causing high concentrations of PM2.5 in each room, followed by cooking, smoking, and cleaning. Door opening time can lead to different interzonal airflows and PM2.5 diffusion rates. By reducing the inner door opening time to less than 1 min, PM2.5 could decrease to 300 μg/m^3. Door closing behavior could decrease risk that PM2.5 diffuses to bedrooms by more than 50%, and exposure of residents in bedrooms could reduce to 100 (μg·h)/m^3 effectively.

Keywords: traditional heating systems; rural dwellings; PM2.5 diffusion; multi-zone network model; daily life behavior; exposure

Citation: Zhang, X.; Yang, Y.; Huang, G.; Chen, B.; Chen, Y.; Zhao, J.R.; Sun, H.J. Diffusion Characteristics of PM2.5 in Rural Dwelling under Different Daily Life Behavior: A Case Study in Rural Shenyang of China. *Buildings* **2022**, *12*, 1223. https://doi.org/10.3390/buildings12081223

Academic Editor: Ricardo M. S. F. Almeida

Received: 29 June 2022
Accepted: 8 August 2022
Published: 12 August 2022

1. Introduction

In recent years, revitalization strategies in rural China have been developed and implemented effectively. However, indoor air quality and pollutant exposure levels in rural dwellings are much higher than those in urban residences in Northeast China, a situation which has been thoroughly studied [1–3]. The main reason for this is that nearly 60% of China's rural residents still rely on burning solid fuels (such as wood, animal manure, charcoal, crop waste and coal) in inefficient and polluting stoves for cooking and heating [4]. Moreover, smoking, cleaning and other daily life behavior could also impact on indoor air quality. According to the World Health Organization, it was estimated that no less than 3.8 million children and adults die every year as a result of household exposure to smoke from dirty cookstoves and fuels [5]. The number of deaths caused by burning solid fuels is as high as 420,000 every year in China [6]. Furthermore, relevant research has proved that indoor PM2.5, which is one of the most harmful pollutants, is exceeding a standard rate as high as 93% in rural houses [7]. However, existing research lacks in-depth analysis of indoor PM2.5 diffusion and exposure assessment in rural houses. Therefore, identifying the mode of PM2.5 changing and its influencing factors is of great significance for improving indoor environmental quality and residents' health in rural houses.

Currently, in order to clarify the changing diffusion mode of PM2.5 in rural dwellings, relevant scholars have done some research on model establishment and concentration

prediction methods. The lumped parameter models based on computational fluid dynamics (CFD) and multi-zone network models were used widely [8]. Relevant studies showed that the models based on CFD were more accurate and intuitive, but the shortcomings were large amounts of calculation, poor convergence, and instability when faced with complex research issues [9–12]. The network model could overcome these limitations. Each network node was connected by air flow paths, and mass and energy conservation equations were established to study air flow, pressure distribution, smoke propagation and pollutant diffusion. Thatcher and Layton [13] calculated indoor PM2.5 concentration distribution by establishing a single-room PM2.5 mass conservation equation in the early 1990s. Li and Chen [14] analyzed the relationship between air exchange rate and penetration rate in a room without a PM2.5 source through theoretical and experimental research. Xie et al. [15] established an indoor PM2.5 prediction model for a single room based on the lumped parameter model in a Chinese dwelling, which could be applied well to predict the indoor particles under different ventilation methods such as natural ventilation and mechanical ventilation. Stewart and Ren [16] developed a zonal model that nested within a multizone model (COMIS) to allow increased resolution in the prediction of local air flow velocities, temperature and PM2.5 concentration distributions between and within rooms. Dimitroulopoulou et al. [17] established an INDAIR model to predict changes in air pollutant concentrations in the British household microenvironment. Under three emission scenarios (no source, cooking, smoking), the model was parameterized by using the probability functions of four pollutants (NO_2, CO, PM10 and PM2.5). The results showed that the model predictive values were consistent with measured data nearly. Shen and Deng [18] established a general model of indoor air quality (IAQ) for natural ventilation buildings. The application was extended from a single room to multiple rooms to predict the impact of PM2.5 on indoor air quality. Zhang and Chen [19] established a variety of mass conservation models for different space layouts to simulate the diffusion behavior of PM2.5 indoors, which laid a foundation for using mass conservation models to study indoor particulate matter diffusion. Fabian et al. [20] used the CONTAM model to predict NO_2 and PM2.5 concentration among low-income families in Boston and emphasized the challenge of simulation due to huge differences in emission intensity. McGrath et al. [21] developed and applied a multi-zone probability calculation model (IAPPEM) based on the INDAIR model, and the results presented that the model could predict PM10 and PM2.5 concentration in a residential indoor environment well. Byung et al. [22] used a CONTAMW simulation to analyze outdoor particle penetration and transport and their impact on indoor air in a multi-zone and multi-story building. The study demonstrated that the CONTAMW simulation could be useful in analyzing the impact of outdoor particles on indoor environments through the identification of key particle transport parameters and validated airflow simulations. Ferro et al. [23] proved that the interior door position and opening angle would affect the change of pollutant concentrations in a remaining functional room caused by short-term indoor emission sources (such as cigarettes, candles, and incense). McGrath et al. [24] determined that the opening of inner doors would cause changes in the interzonal airflows by combining simulation and experimental research. Moreover, it was certificated that opening time would cause a difference in pollutant concentrations in a room. However, the PM2.5 diffusion process and exposure assessment in rural houses has rarely been studied. A multi-zone model was more reliable and convenient than other models for simulating indoor PM2.5 diffusion in multiple rooms in a rural dwelling.

In this paper, the aim was to determine the characteristics of indoor PM2.5 diffusion and residents' exposure under different behaviors of residents in rural dwellings of Northeast China. The contents of this paper are arranged as follows. First, the representative rural house was identified by investigation. A multi-zone network model describing the PM2.5 diffusion characteristics of a representative rural house was established. Moreover, the accuracy of this model was verified through theoretical and experimental research. Finally, the influencing factors of pollution source intensity, indoor airflow, and daily life

behavior on the indoor PM2.5 diffusion process and exposure assessment were discussed and analyzed, which could be a theoretical basis for controlling strategies of indoor PM2.5.

2. Materials and Methods

2.1. Investigations and Measurements

2.1.1. Representative Rural Dwelling

Approximately 246 rural dwellings were investigated in Northeast China from January to March in 2021. Some basic information was recorded, such as building period, orientation, area, residential form, heating system(s), fuel type(s) and so on. The cluster analysis method was used for the selection of representative rural dwellings. Based on the statistical results, different rural dwellings were divided into three classifications by considering some influencing factors [25], as shown in Table 1. Selecting the category with the largest proportion (general dwellings II, 121 households) as the research object. The representative dwelling was identified, as shown in Figure 1. This three-bay house was completed in 2000 and faces south with a construction area of 80 m^2 and a height of 2.7 m. The heating methods were kang (a Chinese traditional radiation heating system) [26] and heating radiators. Wood and straw were usually used for heating and cooking in the kitchen. Two stoves were constructed in the north side. Stove2 was connected with a kang for heating by flue gas and equipped with heating radiators using hot water in the west bedroom and living room. Stove1 was connected with a kang for heating the east bedroom. In order to prevent heat loss, all exterior windows were sealed with plastic film in winter.

Table 1. The clustering analysis of households' characteristics.

Subject (Unit)	Classification			Clustering		Error		F	Sig. (≤0.05)
	I	II	III	Mean Square	df	Mean Square	df		
Number of permanent residents (Person)	5	3~5	2	80.72	2	0.67	243	120.67	0.000
Residents' age (Years)	20~70 3~18	20~70 3~18	50~79	2691.76	2	186.45	243	14.44	0.000
Annual income of a household (Yuan)	81,290	47,990	21,888	5.87×10^{10}	2	1.07×10^{8}	243	546.96	0.000
Building area (m^2)	114	82	76	14,854.64	2	877.68	243	16.93	0.000
Plan layout	Four-bay	Three-bay	Two-bay						
Heat transfer coefficient of exterior wall ($W/(m^2 \cdot K)$)	1.4	1.4	1.5	0.72	2	0.10	243	6.94	0.001
Households (Number)	31	121	94						

2.1.2. Measurements

During heating and cooking periods, smoke and pollutants are generated by fuel combustion in stoves and discharged to the outside through chimneys. Some of the smoke and pollutants are discharged from the kitchen to other functional rooms and outdoors via doors and gaps in building envelopes. In order to discuss the spatiotemporal variation characteristics of indoor PM2.5 in traditional dwellings of Shenyang, China, instruments for measuring temperature, relative humidity and PM10, PM2.5, CO_2 concentration were set for continuous monitoring and placed in the center of each functional room, including the bedrooms, corridor, living room, and kitchen. The magnetic switch recorder measured the opening time of doors (opening time per instance) and frequency in residents' daily life, and the test probes were arranged on the doors, as shown in Figure 2. The testing instruments and their accuracy are shown in Table 2. Among them, a PM2.5 testing recorder had been corrected with TSI AM510 before doing experiments. The CO_2 concentration, temperature and humidity recorders were set to record data every two minutes, and the door-opening frequency, PM10 and PM2.5 recorders were set to record data every minute. The measuring period was on 13–19 January 2020. Outdoor wind speed and direction were

also measured. The height of the testing point outside the house is 1.5 m above on the ground. The mean wind speed was 0.2 m/s, and the main wind direction was E and SE. Residents living in the representative rural dwelling include one older woman (70 years old), two middle-aged men (45 years old), and one young boy (12 years old). Experimental conditions are shown in Table 3. The experimental parameters are as follows. First, the daily life behavior of residents in this research included heating, cooking, smoking, cleaning, and ventilating. Second, daily life behaviors were carried out at different times and positions between January 13th and 19th, respectively. Heating and cooking were in the kitchen, smoking was in the living room, and cleaning behavior was in the east bedroom. Third, during the testing process, all of the windows were closed, and ventilating behavior was reflected by random opening of the exterior door and interior doors.

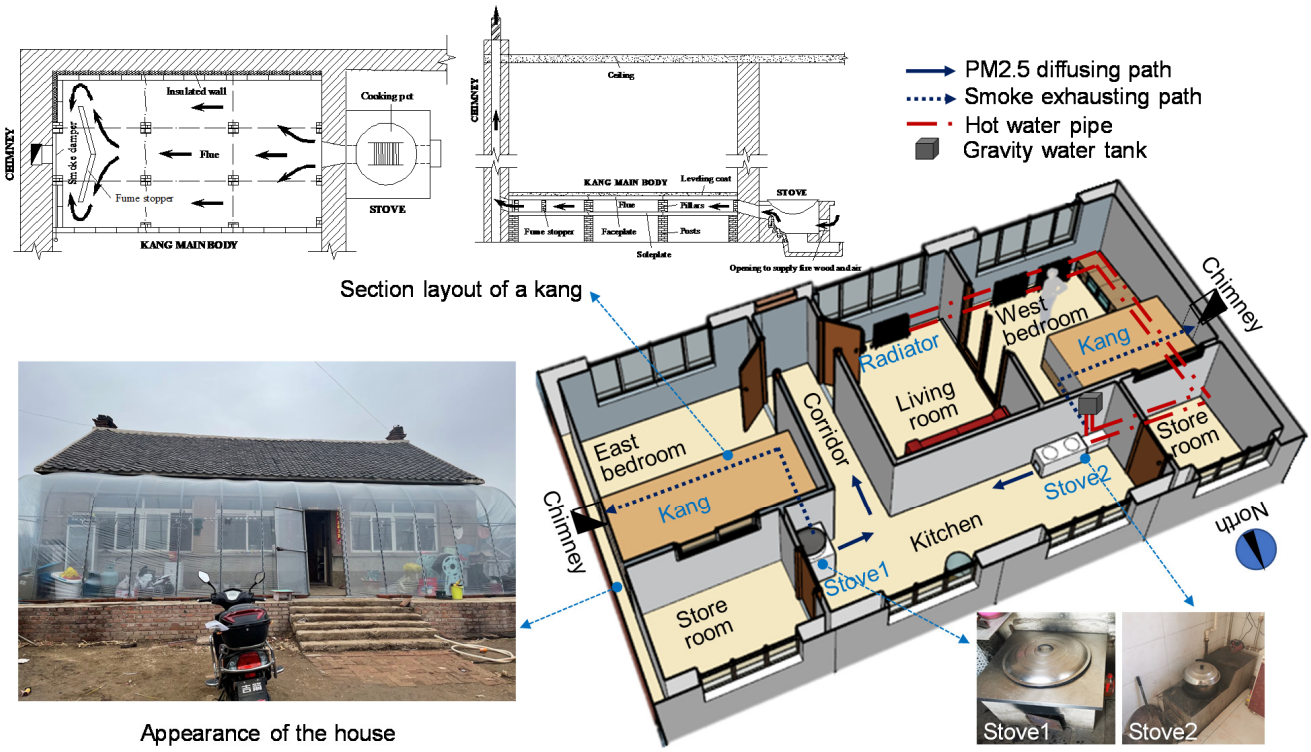

Figure 1. Appearance of the representative rural house and a diagram of a kang and stove.

Table 2. Testing instruments and their measurement accuracy.

Test Parameters	Test Instruments	Instrument Precisions	Manufacturers
Air temperature Relative humidity	Air temperature and relative humidity recorder WEZY-2	−40–100 °C (±0.1 °C) 0–100% RH (±0.1% RH)	TIAN JIAN HUA YI Technology Co., Ltd.
PM10 and PM2.5 concentration	PM2.5 recorder developed based on Plan tower a003 sensor ZF-R3	0–2999 μg/m^3 ±1 μg/m^3	BEIJING CO-CLOUD www.co-cloud.com.cn Beijing, China (accessed on 1 January 2020)
CO_2 concentration	CO_2 recorder WEZY-1	0–5000 ppm ±75 ppm	TIAN JIAN HUA YI Technology Co., Ltd.
Door switching frequency	Magnetic switch recorder CKJM-1	Maximum sensing distance 30 mm	TIAN JIAN HUA YI Technology Co., Ltd.

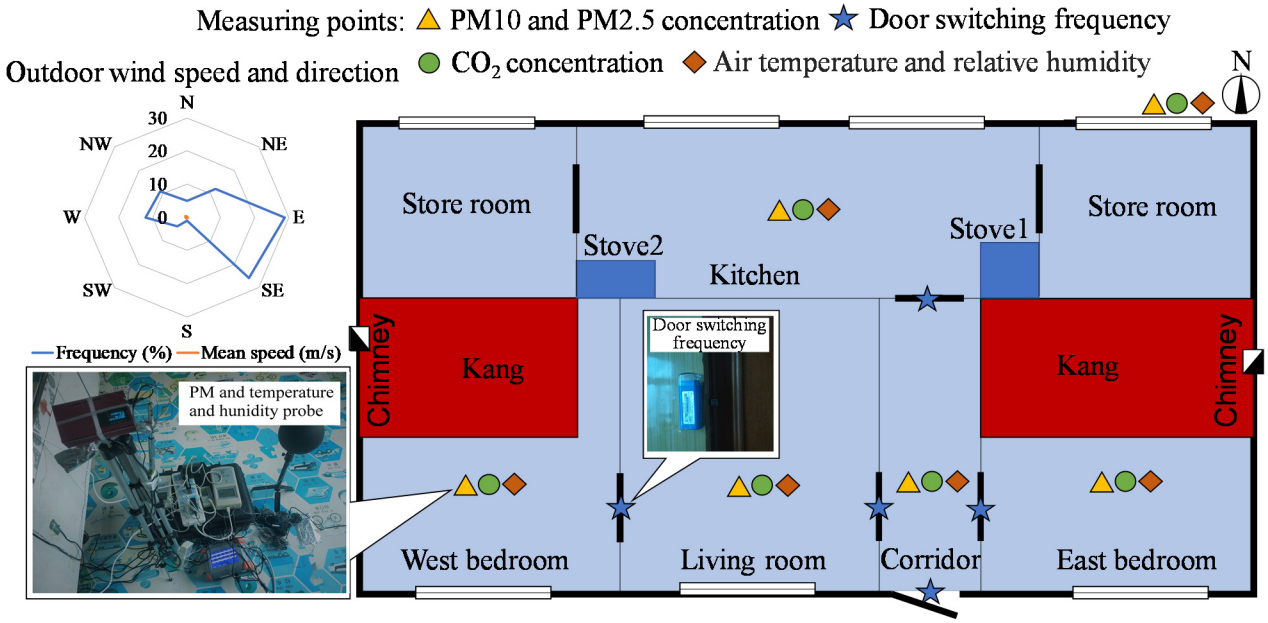

Figure 2. Instruments' arrangement and measuring points.

Table 3. Measuring conditions.

Date	Time	Fuel Consumption (Straw/Wood)	
		West Stove (kg)	East Stove (kg)
13st, JAN.	7:20	0.03/9.5	0.02/10.8
	14:00	0.02/12.4	0.02/12.0
14st, JAN.	7:34	0.03/11.8	0.03/10.5
	14:10	0.02/12.5	0.02/12.3
15st, JAN.	7:35	0.02/10.8	0.02/11.0
	14:00	0.02/12.3	0.02/12.0

The random error was solved by t-distribution method at a given confidence level of 95%, and the systematic error was solved by square and root compound method. Finally, these two were combined for analysis [27]. The system error was calculated according to Formula (1):

$$B_{a,sys} = LC \times FS \quad (1)$$

where, $B_{a,sys}$ is the system error; LC is the accuracy level of the measuring instrument; FS is the measuring instrument range.

The random error was calculated according to Formulas (2) and (3):

$$B_{a,ran} = t\sigma'/\sqrt{N} \quad (2)$$

$$\sigma' = \left[1/(N-1) \times \sum_{j=1}^{N} (Y_j - Y_{ave})^2\right]^{0.5} \quad (3)$$

where, $B_{a,ran}$ is random error; σ' is the sample variance; N is the number of samples; t is the critical value of t distribution, determined by samples and the confidence level of the experimental test; Y_j is a single measurement value; Y_{ave} is an average measurement value.

According to Formulas (1) and (2), the total measurement error of the direct measurement parameters was calculated by Formula (4):

$$B_a = \sqrt{B_{a,sys}^2 + B_{a,ran}^2} \quad (4)$$

The total measurement errors were: PM2.5: 3.47 μg/m^3, CO_2: 4.77 ppm.

2.1.3. Particulate Matters Variations

In order to clarify source intensity and diffusion characteristics of indoor PM2.5 and to verify the calculation accuracy of the PM2.5 diffusion model, experiments were conducted in the representative rural dwelling. Some measured results are shown in Figure 3. Indoor PM2.5 and PM10 concentrations during cooking and heating were far beyond the national standard of 75 μg/m^3 [28] most of the time, except 0:00–5:00 in each day. As cooking and heating behaviors were carried out in the kitchen, the PM2.5 concentration of each room increased rapidly. As shown in Figure 3c,d, the peak concentrations of PM2.5 and PM10 in bedrooms were generated following 20 min after those in the kitchen. This illustrates that pollutants can diffuse into other functional rooms within a limited time. Figure 3e shows that the concentrations of PM2.5 and PM10 had no correlation in the kitchen. The emission time of PM2.5 was about 30 min (7:30–8:00). The varied concentrations of PM2.5 were distributed exponentially. The fitting results ($R^2 > 0.9$) are shown in Figure 3f. The mean concentration of PM2.5 was 900 μg/m^3, which can be used for calculating the mean emission rate. Figure 3g,h show little difference in temperature and humidity in these three days.

2.2. Simulations

2.2.1. Model Establishment

Indoor PM2.5 was taken as the main research object, Therefore, a PM2.5 diffusion model was established based on a geometric model (shown in Figure 4).

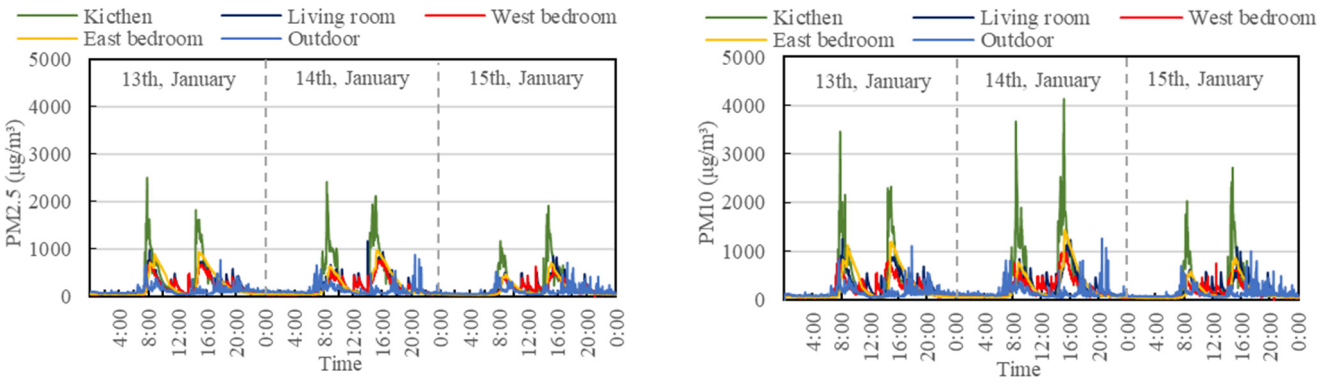

(**a**) (**b**)

Figure 3. *Cont.*

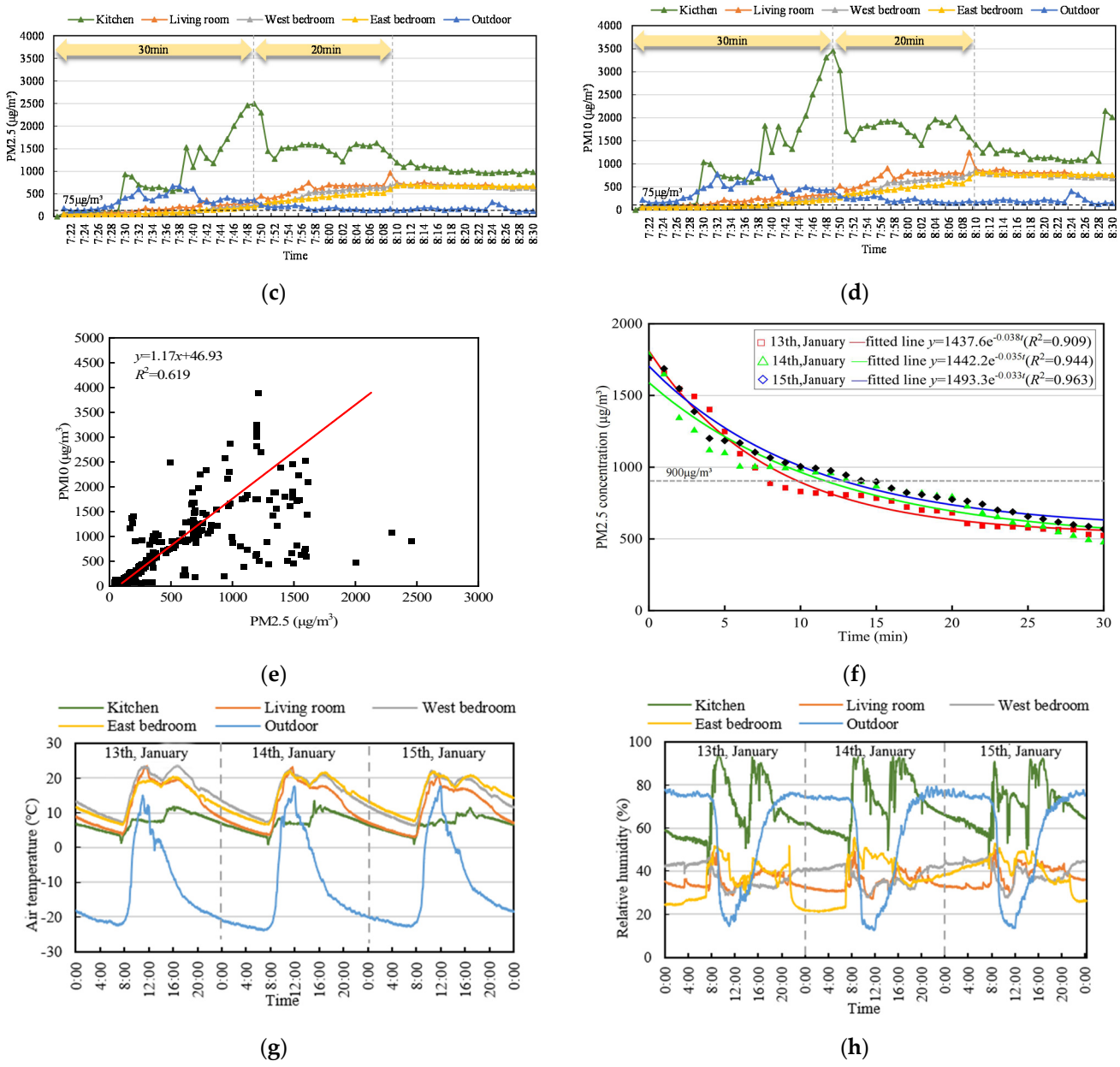

Figure 3. Indoor and outdoor PM variation ((**a**) PM2.5 variation during 13–15 January; (**b**) PM10 variation during 13–15 January; (**c**) indoor and outdoor PM2.5 variation during heating and cooking; (**d**) indoor and outdoor PM10 variation during heating and cooking; (**e**) relationship between PM2.5 and PM10 in the kitchen; (**f**) the fitting results of PM2.5 source intensity during heating; (**g**) indoor and outdoor air temperature; (**h**) indoor and outdoor air relative humidity).

Indoor PM2.5 diffusion model was established as Formula (5):

$$V\frac{dC_i}{dt} = E - (Q_0 + KV)C_i - \sum_{k=1}^{n} Q_{ik}(C_i - C_k) + pQ_sC_i \quad (5)$$

$$Q_{21} + Q_{01} = Q_{12} + Q_{10} \quad (6)$$

$$Q_{12} + Q_{32} + Q_{02} = Q_{21} + Q_{23} + Q_{20} \quad (7)$$

$$Q_{23} + Q_{43} + Q_{53} + Q_{03} = Q_{32} + Q_{34} + Q_{35} + Q_{30} \quad (8)$$

$$Q_{34} + Q_{04} = Q_{43} + Q_{40} \quad (9)$$

$$Q_{35} + Q_{05} = Q_{53} + Q_{50} \tag{10}$$

where, V is the room volume, m^3; Q_f is the infiltration fresh air volume from the outdoors, m^3/h; Q_s is the infiltration air volume through building envelope, m^3/h; p is the PM2.5 penetration rate, 1/h; E is the indoor PM2.5 emission rate, μg /h; Q_o is the air flow to the outdoors, m^3/h; K is the PM2.5 deposition rate, 1/h; Q_{ik} is the interzonal airflow representing the transport of pollutants between internal compartments, m^3/h; C_i is the PM2.5 mass concentration of room i, $\mu g/m^3$; C_o is the outdoor PM2.5 mass concentration, $\mu g/m^3$; C_k is the PM2.5 mass concentration of room k, $\mu g/m^3$; t is time, h; $k = 1, 2 \ldots$ n; Q is the interzonal airflow, which was calculated with CO_2 tracer gas method, m^3/h.

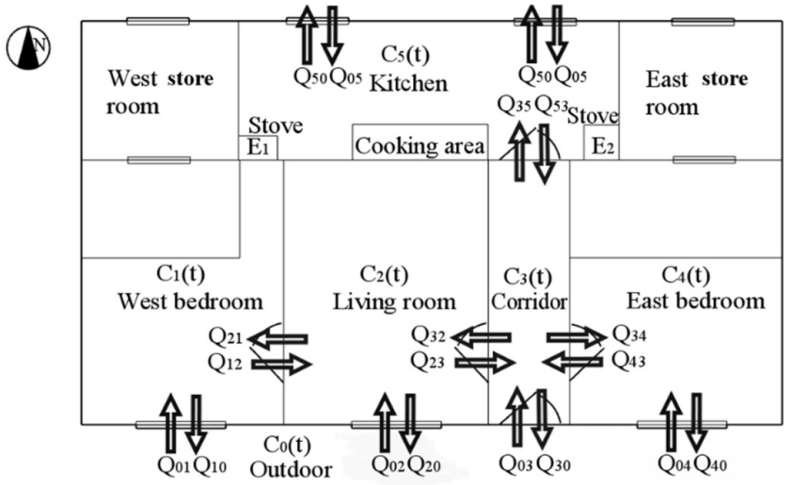

Figure 4. Indoor PM2.5 diffusion model.

During the diffusion model establishment process, it was assumed that only the west stove E_1 was used for heating. According to indoor PM2.5 mass conservation, the indoor PM2.5 diffusion model of the rural dwelling was simplified as Formulas (11)–(15). Among them, PM2.5 emission source intensity and interzonal airflow were the main influencing factors of PM2.5 diffusion.

$$V_1 \frac{dC_1(t)}{dt} = Q_{21}(C_2(t) - C_1(t)) - Q_{10}C_1(t) - KV_1C_1(t) \tag{11}$$

$$V_2 \frac{dC_2(t)}{dt} = Q_{21}(C_1(t) - C_2(t)) + Q_{32}(C_3(t) - C_2(t)) - Q_{20}C_2(t) - KV_2C_2(t) \tag{12}$$

$$V_3 \frac{dC_3(t)}{dt} = Q_{32}(C_2(t) - C_3(t)) + Q_{34}(C_4(t) - C_3(t)) + Q_{53}(C_5(t) - C_3(t)) - (Q_{30} + KV_3)C_3(t) \tag{13}$$

$$V_4 \frac{dC_4(t)}{dt} = Q_{34}(C_3(t) - C_4(t)) - Q_{40}C_4(t) - KV_4C_4(t) \tag{14}$$

$$V_5 \frac{dC_5(t)}{dt} = Q_{53}(C_3(t) - C_5(t)) + E_1 - Q_{50}C_5(t) - KV_5C_5(t) \tag{15}$$

2.2.2. Parameters Settings

(1) Assuming conditions

a. The research rural dwelling was taken as a control system. Each room was taken as a control body (or network node). Indoor air was mixed fully in each control body. Each network node was connected by air flow paths [17].

b. The indoor air temperature and relative humidity, pollutant concentrations, and pressure of each functional room were uniform.

c. As shown in Figure 3a, cooking and heating occured in the kitchen, the concentration of indoor PM2.5 is always higher than that outdoors, and the impact of outdoor PM2.5 on

indoor PM2.5 is very a little. As the airflow was bidirectional; it is assumed that a high concentration of PM2.5 was generated in the kitchen and discharged to the outside through building envelopes. Then, "$-pQ_sC_i$" was used for simulated calculation.

d. Since the airflow was bidirectional, it was believed that a high concentration of PM2.5 generated in the kitchen was discharged to the outdoors through building envelopes. The influence of flue gas density change could be ignored [18].

e. Particles' transformation, condensation, volatilization, atomization, and resuspension had little effect on PM2.5 concentration, and could be ignored [29].

f. Due to the small particle size of PM2.5, its diffusion in the farmhouse is carried out in the turbulent flow field, assuming that the PM2.5 carried by the airflow has no effect on the characteristics of the fluid masses, and that the diffusion of PM2.5 is entirely caused by the mixing between the fluid masses carrying PM2.5.

(2) Initial concentrations

The initial concentration of PM2.5 in each room was obtained through continuous monitoring (kitchen: 65 μg/m^3, corridor: 85 μg/m^3, living room: 75 μg/m^3, west bedroom: 75 μg/m^3, east bedroom: 76 μg/m^3), which was measured on 17 January.

(3) Source intensity

This study compared the calculated results of the fitted PM2.5 emission source intensity and the mean emission rate. Among them, $\overline{E}$ [29] was calculated based on Formula (16), and the results are listed in Table 4:

$$\overline{E} = V \times \left[\frac{C_{it} - C_{i0}}{\Delta T} + \overline{(\alpha + K)} \times \overline{C_i} - \alpha \times C_{i0} \right] \quad (16)$$

where, $\overline{E}$ is the mean emission rate of PM2.5; C_{it} is the PM2.5 mass concentration of room i at time t, μg/m^3; C_{i0} is the PM2.5 mass concentration of room i at the initial moment, μg/m^3; $\overline{C_i}$ is the PM2.5 mean mass concentration of room i in time ΔT interval, μg/m^3; α is the air exchange rate, h^{-1}; As all the doors and windows were sealed by plastic films, the air exchange rate $\alpha = 0$ h^{-1}.

Table 4. Source intensity of different PM2.5 emissions.

Different Behavior	Location	PM2.5 Concentration (μg/m^3)			Mean Emission Rate (μg/min)	Fitted Exponential Function	R^2	Duration (min)
		Peak	Mean ± SD	Final				
Heating	Kitchen	1759	873.4 ± 356.0	525	1455.5	$y = 1437.6e^{-0.038t}$	0.909	30
Cooking	Kitchen	1309	859.6 ± 312.7	521	1274.0	$y = 1206.0e^{-0.063t}$	0.960	15
Smoking	Living room	761	425.7 ± 238.4	343	1020.3	$y = 571.2e^{-0.052t}$	0.901	10
Cleaning	East bedroom	185	122.5 ± 59.6	84	333.5	$y = 228.5e^{-0.194t}$	0.980	5

PM2.5 emission intensity under different daily life behavior and fitted exponential functions ($R^2 > 0.9$) is presented inTable 4. As can be seen, there were obvious differences between results of PM2.5 concentration, mean emission rate and duration. Heating in the kitchen was the highest at 1759 μg/m^3; the mean emission rate was 1455.5 μg/min.

(4) Interzonal airflow

The interzonal airflow was obtained with the CO_2 tracer gas method [30], and the limited value of CO_2 concentration is 1000 ppm [31]. The interzonal airflow could be calculated according to Formula (17):

$$Q = \frac{V}{t} \times \ln \frac{C_{i0}}{C_{it}} \quad (17)$$

where, C_{it} is the CO_2 volume concentration of room i at time t, ppm; C_{i0} is the CO_2 volume concentration of room i at the initial moment, ppm.

As shown in Figure 5a, the concentration difference of CO_2 was changed little every day. The exterior door and inner door of kitchen were opened for exhausting flue gas and particles, and much fresh airflow caused the CO_2 concentration to decay faster in the

kitchen and corridor. As special living habits of rural residents were carried out in different functional room, the inner doors were opened frequently (Figure 5b,c). The interzonal airflow calculated results are shown in Figure 5d. As can be seen, when the exterior door and the interior door of kitchen were opened, the airflow was as high as 110 m^3/h at the exterior door, and the airflow at the interior door of the kitchen was about 46 m^3/h. While opening the door of bedroom and living room, the airflow was about 34 m^3/h. Among them, the infiltration air volume was as follows: $Q_{10} = Q_{20} = Q_{40} = 4.4$ m^3/h, $Q_{50} = 3.3$ m^3/h.

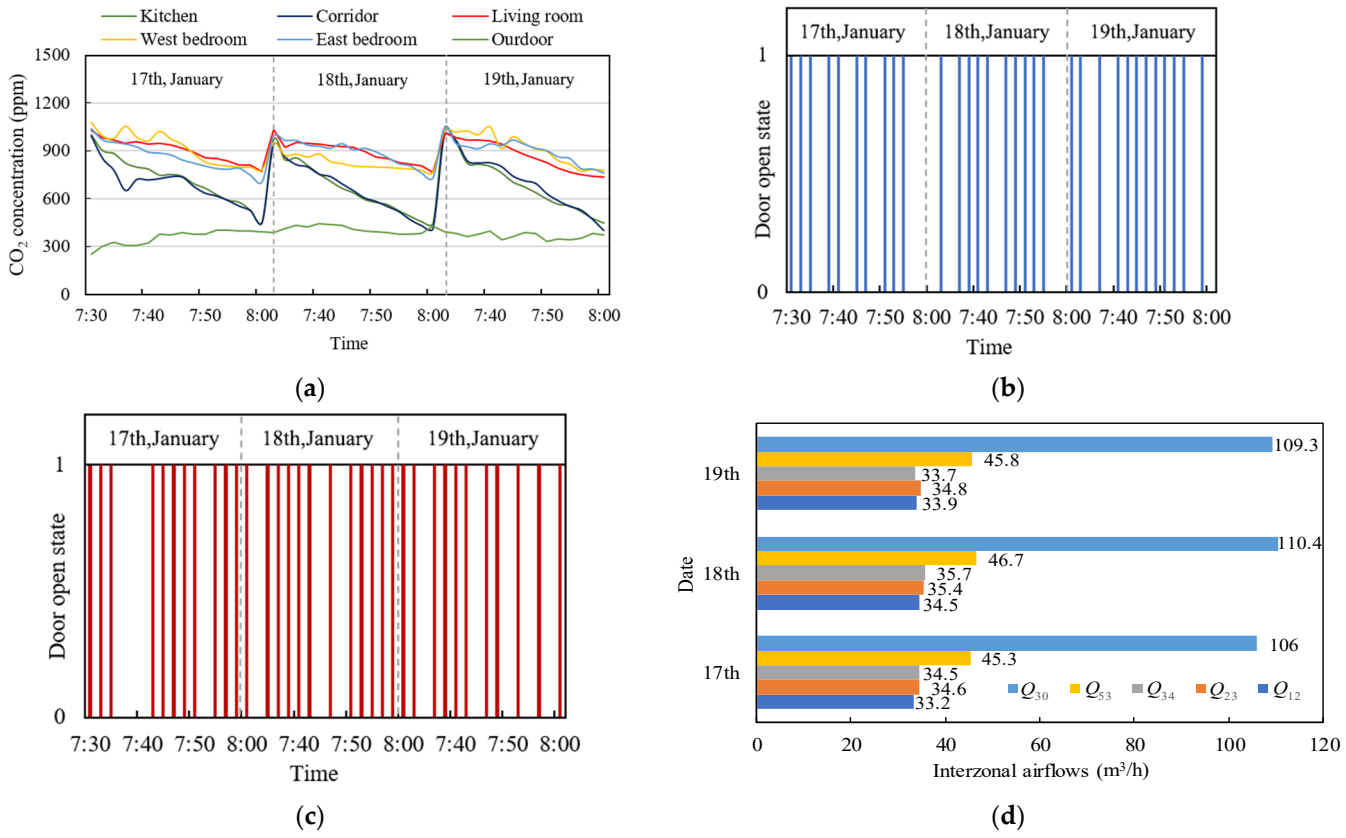

Figure 5. The changes of CO_2 concentration and door opened states during the heating process ((**a**) the changes of CO_2 concentration; (**b**) the door of the living room opened state; (**c**) the door of the east bedroom opened state, where 1 represents closed, 0 represents opened; (**d**) interzonal airflow in each room).

(5) Deposition rate

Byrne et al. [32], Fogh et al. [33] and Thatcher et al. [34] tested more than 100 dwellings and obtained deposition rates of PM10 and PM2.5 of 1.0 h^{-1} and 0.4 h^{-1}, respectively, through the combination of theory and experiment. Xie et al. [15] determined that the PM2.5 deposition rate in Chinese residential dwellings was 0.3–0.69 h^{-1} through experimental research, with a median of 0.45 h^{-1}. Comparing with the theoretical calculation value (0.38 h^{-1}), the error is 16%. In this study, the deposition rate was calculated to be 0.33–0.47 h^{-1} by the deposition model of indoor PM2.5 [35] in the rural dwelling, which was mostly consistent with previous studies. The deposition rate of PM2.5 was set to 0.4 h^{-1}.

(6) Penetration factor

Liu and Nazaroff [36] tested the penetration factor of particles with different sizes separately under various pressure differential conditions in an environmental chamber. The results showed that the particle size, gap height, gap depth, pressure difference and material had a greater impact on the penetration factor of particles. When the pressure difference

between the two ends of the gap was greater than 4 Pa and the gap height was greater than 1 mm, the penetration factor p in the size range of 0.02~7 μm was approximately 1. In this study, the penetration factor of PM2.5 was set to 1.

2.2.3. Model Accuracy

Calculated results were compared with measured results in Figure 6. As can be seen, the relative errors between calculated results by multi-zone network model and experimental results are within 10%. Therefore, PM2.5 diffusion in a rural dwelling can be predicted. Furthermore, the impacts of daily life behavior on PM2.5 diffusion can be analyzed and discussed.

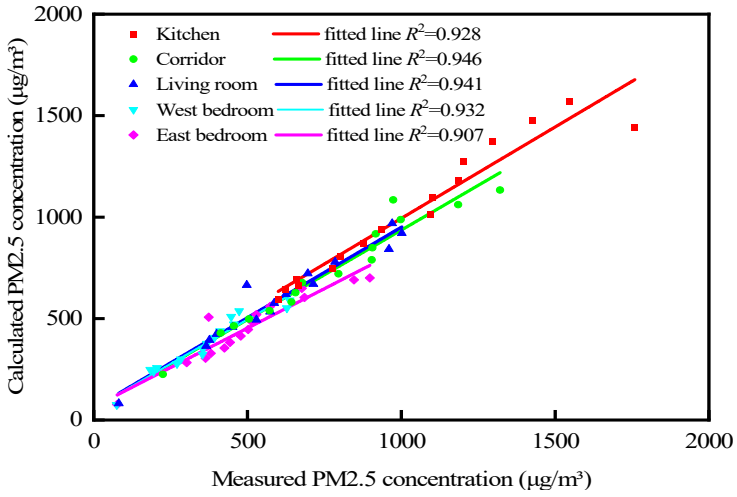

Figure 6. Calculated values compared with measured values.

3. Results

3.1. Impact of Different Behavior on PM2.5 Diffusion

The concentrations of PM2.5 in each functional room under different behaviors are shown in Figure 7. It indicates that PM2.5 concentration exceeded 75 μg/m^3 in each room. PM2.5 generated by smoking in living room can only impact on the adjacent room (the west bedroom) by opening the inner doors. Cleaning (the peak value is only 185 μg/m^3) in the east bedroom could not impact adjacent rooms. However, under the condition of heating, as the concentration of PM2.5 in kitchen was highest at 1559 μg/m^3, the average diffusion rate from the source to each room was reduced from 17.7 μg/(m^3·min) to 10.1 μg/(m^3·min). While cooking was occurring in the kitchen, the peak concentration of PM2.5 was 1059 μg/m^3, and the average diffusion rate from the source to each room was reduced from 6.9 μg/(m^3·min) to 3.5 μg/(m^3·min). This illustrates that when the PM2.5 concentration of the pollution source was decreased by 500 μg/m^3, the diffusion rate from the source to each room could decrease by three times.

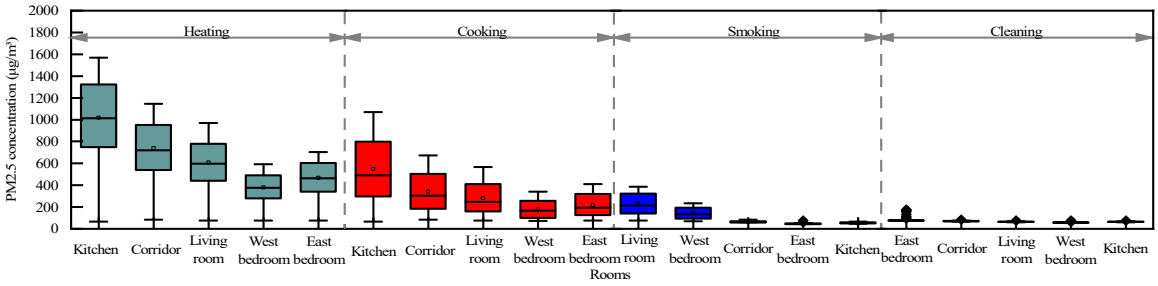

Figure 7. Simulation results of PM2.5 concentration during different behaviors in the dwelling.

3.2. Impact of Door Opening Time on PM2.5 Diffusion

Based on a lot of investigations in Shenyang rural dwellings, during heating, the exterior door and interior door of the kitchen were opened fully, and the interior door of store rooms were closed. The opening of other interior doors was random. The opening time of different interior doors can lead to variations in interzonal airflow. The calculated results are shown in Figure 8. The airflow of the exterior door was constant at 106 m^3/h. However, the airflow of interior doors was variable from 4.8 m^3/h to 72.7 m^3/h. Moreover, the simulated concentration of PM2.5 under different interior door opening is presented in Figure 9. When the interior doors of the bedrooms and living room were closed, PM2.5 was difficult to diffuse to other rooms, which lead to higher concentrations of PM2.5 in the kitchen and corridor. However, in the bedrooms and living room, concentrations of PM2.5 increased as the opening time increased gradually. When the opening time reached more than 5 min, the interzonal airflow could be changed a little. PM2.5 concentrations were steady. It was also shown that reducing the opening time of inner doors to be less than 1 min could decrease PM2.5 concentrations to less than 300 $\mu g/m^3$.

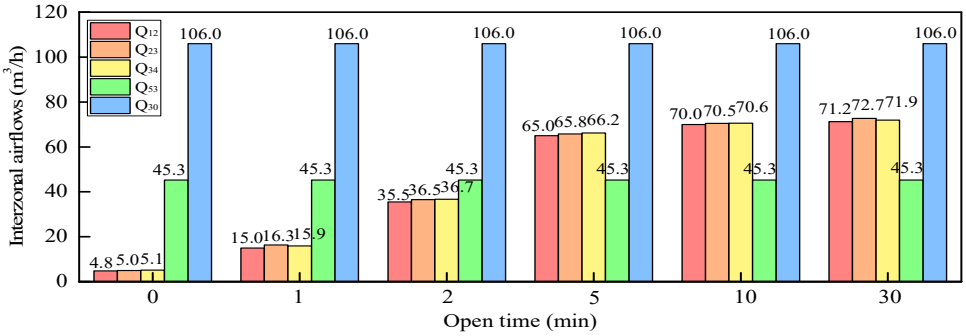

Figure 8. Interzonal airflows under different door-opening times (Where 0 min represents closed, 30 min represents all doors are opened fully during heating process).

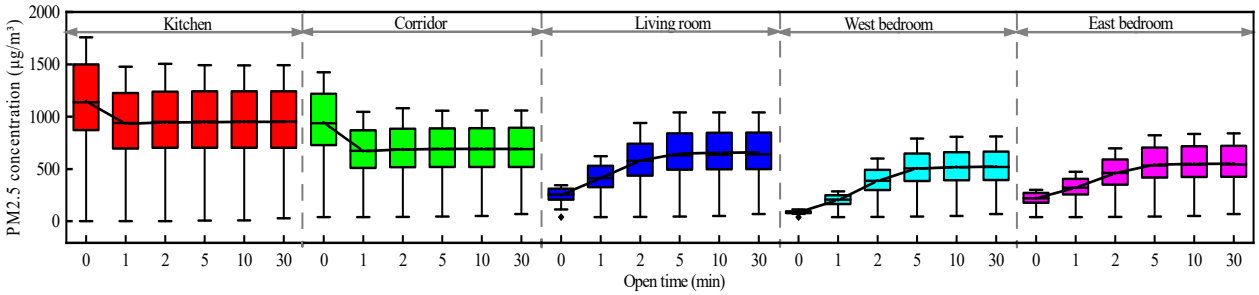

Figure 9. Simulated concentration of PM2.5 under different door-opening times.

Figure 10a shows the changes of PM2.5 concentration in each room. When the opening time was 6 mins, PM2.5 concentrations of each room could reach peak values. PM2.5 concentrations were 200–300 $\mu g/m^3$ in each room. While all doors were closed, the PM2.5 concentrations in the bedrooms and living room could reduce to less than 100 $\mu g/m^3$ (shown in Figure 10b). However, most PM2.5 accumulated in the kitchen, with the peak concentration the highest at 2300 $\mu g/m^3$. This illustrates that by only closing the interior doors of the bedrooms and living room, indoor PM2.5 would diffuse to the bedrooms and living room through the gaps in interior doors. In conclusion, door closing behavior could decrease PM2.5 difusion to other rooms by more than 50%.

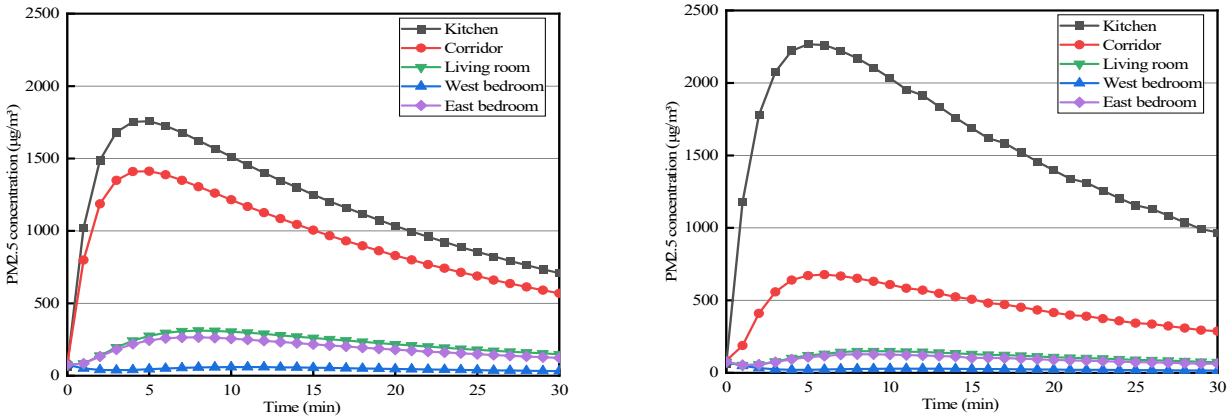

Figure 10. The changes of PM2.5 concentration in each room ((**a**) the interior doors to the bedrooms and living room were closed, the exterior door and interior door to the kitchen were opened fully; (**b**) all doors were closed).

3.3. Indoor PM2.5 Exposure

Borrego et al. [37] pointed out that the time–activity model is one of the most common and effective human exposure evaluation methods through experimental research. As on-site monitoring is time-consuming and labor-intensive, the PM2.5 diffusion model and residents' behaviors are combined to establish a PM2.5 exposure model [38] to calculate the exposure of residents under different daily life behaviors in this study. The indoor behaviors of different age groups (older women (70), middle-aged men (45) and young men (12)) were tracked in the test house under the influence of different pollution sources. This is presented in Table 5.

Table 5. Activity intensity of different age groups.

Different Behavior	Location			Activity Intensity (IR(t), m^3/h)		
	Old	Middle-Aged	Young	Old	Middle-Aged	Young
Heating	Kitchen	Kitchen	East bedroom	Mild activity (0.456)	Mild activity (0.558)	Rest (0.3)
Cooking	Kitchen	Kitchen	East bedroom	Mild activity (0.456)	Mild activity (0.558)	Rest (0.3)
Smoking	East bedroom	Living room	West bedroom	Rest (0.306)	Light activity (0.444)	Light activity (0.4)
Cleaning	East bedroom	West bedroom	Living room	Mild activity (0.366)	Light activity (0.444)	Light activity (0.4)

IR(t) is the respiratory rate, which is related to age, gender, activity intensity, etc. [39].

The calculated results of exposure and potential dose of residents under different behaviors are shown in Figure 11. The PM2.5 exposure of older women and middle-aged men was the largest during the heating process, which was 431.7 μg·h/m^3. Moreover, the middle-aged respiratory rate was larger, and its potential dose was the largest at 240.9 μg, which was higher than that of the older adult. While the young boy was in the bedroom, his exposure was the smallest at 170.4 μg·h/m^3, and the potential dose was 51.1 μg. However, during smoking, the smoker himself was the most harmed. At the same time, it had a certain impact on the young boy who smoked second-hand smoke. During cleaning, due to its lower pollution intensity, there was the lowest impact on residents' exposure and potential dose.

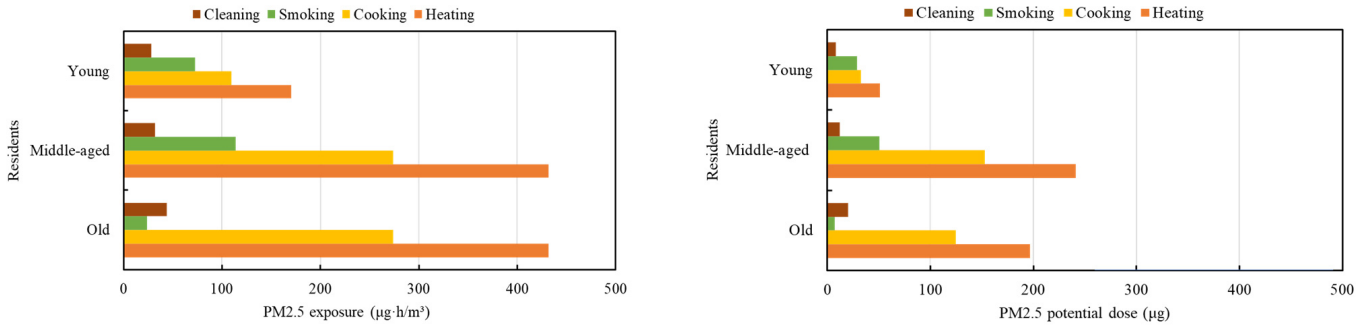

(**a**) (**b**)

Figure 11. Exposure of residents under different behaviors ((**a**) exposure, (**b**) potential dose).

Figure 12 presents the calculation results of exposure and potential dose to residents under different door opening times during the heating process. The PM2.5 exposure and potential dose of the young boy who was in the east bedroom decreased significantly with the reduction of the door opening time. However, for elderly women and middle-aged men who were doing something in kitchen, the PM2.5 exposure (480.7 μg·h/m^3) and potential doses were the lowest (219.2 μg, 268.2 μg) when the door was opened for 1 min. With the inner doors closed, PM2.5 was difficult to diffuse to other rooms, and the PM2.5 exposure and potential dose of the young boy were the lowest (94.4 μg·h/m^3, 28.3 μg). However, it seriously endangered the older women and middle-aged men who were active in kitchen. The exposure was 591.6 μg·h/m^3, and the potential dose was between 269.8 μg and 330.1 μg.

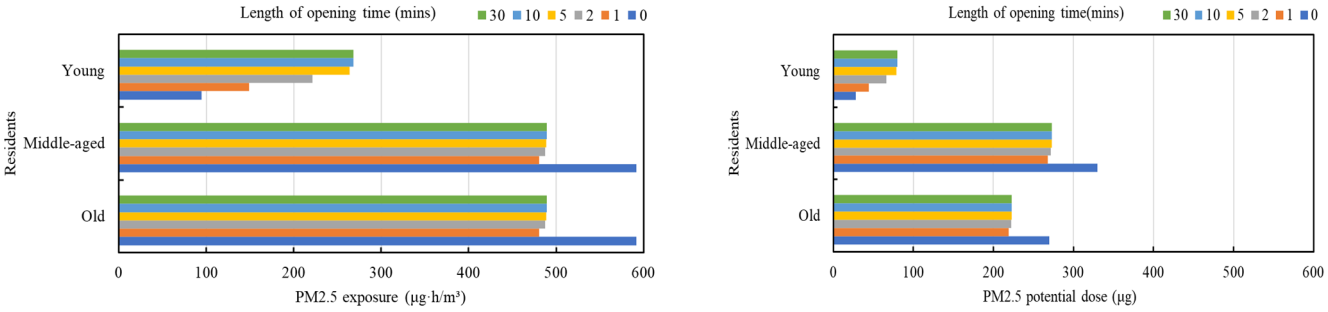

(**a**) (**b**)

Figure 12. Exposure of residents under different door opening behaviors in different rooms ((**a**) exposure, (**b**) potential dose).

4. Discussion

Currently, the multi-zone network model has been used widely to predict the particulate matters variations of single dwellings in other countries. However, due to the lack of experimental data, numerous studies set the PM2.5 emission source intensity as a constant value [17,20,21]. The mean emission rate was used for simulation calculation. Figure 13 presents the changes of PM2.5 concentration in each room calculated by the fitted emission intensity and mean emission rate, respectively. As can be seen, the PM2.5 concentration calculated by the mean emission rate (Figure 13b) had a steady trend after rising to the peak concentration, which overestimated indoor PM2.5 concentration noticeably, and the errors were large. On the contrary, the results calculated by the fitted emission intensity had a better goodness-of-fit with the experimental data.

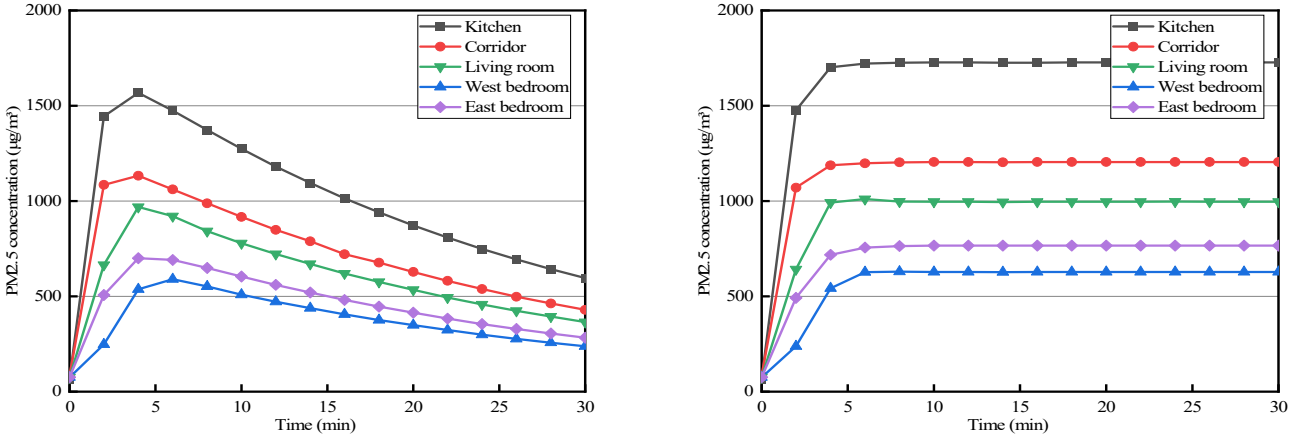

Figure 13. Simulated concentration of PM2.5 in each room by different methods ((**a**) adopted the fitted emission intensity; (**b**) adopted the mean emission rate).

In addition, PM2.5 emission source intensity measuring results were compared at home and abroad. It was found that the results of smoking and cleaning behaviors were similar to those results measured by Jiang et al. [40] and Aquilina and Camilleri [41], according to which the PM2.5 emission rates were 1600 ± 470 μg/min (smoking) and 242.7 μg/min (cleaning). For cooking behavior, it has been proved that the oil fume components and PM2.5 emission characteristics were related to cooking methods, edible oil types and oil temperature closely through simulation and experimental research [42,43]. As a result, the PM2.5 emission rates and duration (1274 μg/min, 15 min) tested in this research were quite different from the results of He et al. [44] (2680 ± 2180 μg/min, 8 min). Heating behavior was concerning as a unique and primary source of PM2.5 in rural dwellings. It was found that the study results had large deviations due to differences in fuel consumption and types, combustion efficiency, stove types, indoor and outdoor environments, ventilation methods, etc. [45–48]. The PM2.5 emission source intensity needs more follow-up and detailed research during the heating process.

5. Conclusions

In rural dwellings of Northeast China, the changing rule and main influencing factors of indoor PM2.5 concentration were clarified by establishing a multi-zone network model. PM2.5 exposure assessment of residents in a rural dwelling were calculated and analyzed by a PM2.5 exposure model. Some conclusions are shown as follows:

(1) The relative errors between theoretical results calculated by the multi-zone network model and the experimental results are within 10%, which verifies the accuracy of the established model. Therefore, this model can predict diffusion characteristics of PM2.5 under different daily life behaviors in rural dwellings.

(2) PM2.5 concentrations during heating behaviors in the kitchen was the highest at 1759 μg/m^3, and the average diffusion rate from the source to each room was reduced from 17.7 μg/(m^3·min) to 10.1 μg/(m^3·min). Through comparative analysis, when the PM2.5 concentration of the pollution source was decreased by 500 μg/m^3, the diffusion rate from the source to each room could decrease by 3 times.

(3) Door opening time can lead to different interzonal airflow and PM2.5 diffusion rate. Reducing the interior door opening time to less than 1 min could decrease PM2.5 concentration to 300 μg/m^3. Door closing behaviors could decrease PM2.5 diffusion to other rooms by more than 50% effectively.

(4) The PM2.5 exposure model is suitable for PM2.5 short-term exposure assessment of residents. The potential dose of the middle-aged men during the heating process was the largest at 240.9 μg. While the interior doors were closed, the exposure of residents in the

kitchen was the highest at 591.6 (μg·h)/m^3, and the exposure of residents in the bedrooms could reduce to 100 (μg·h)/m^3 effectively.

(5) In order to reduce the risk of PM2.5 exposure to rural residents and to slow the spread of PM2.5 generated by pollution sources to various functional rooms, it is possible to consider the development and use of some clean energy sources to reduce the intensity of PM2.5 emission sources; frequent closing of doors or reducing the length of opening time of interior doors by residents in their daily lives; and mechanical smoke extraction can be used, such as lower economic cost fans and range hoods.

Author Contributions: X.Z. and Y.Y. designed the study; X.Z. conducted the data analyses and wrote the first draft of the manuscript; G.H., Y.Y. conducted some experiments and simulations; B.C. provided some suggestions on the process of doing experiments and writing; Y.C. provided some suggestions on simulations and some comments on the "Introduction"; J.R.Z. and H.J.S. contributed to the data verification, adjustment of results, discussions and revisions. All authors have read and agreed to the published version of the manuscript.

Funding: This research received no external funding.

Institutional Review Board Statement: Not applicable.

Acknowledgments: This work was supported by the National Nature Science Foundation of China (No. 52078098 and No. 51608092), and National Science Foundation of Liaoning Province (No. 2019-ZD-0022). The authors would like to thank the survey participants to carry out this research.

Conflicts of Interest: The authors declare no conflict of interest.

References

1. Lan, Q.; Chapman, R.S.; Schreinemachers, D.M.; Tian, L.; He, X. Household stove improvement and risk of lung cancer in Xuanwei. *China J. Natl. Cancer Inst.* **2002**, *94*, 826–835. [CrossRef]
2. Shen, G.F.; Wang, W.; Yang, Y.F.; Ding, J.N.; Xue, M.; Min, Y.J.; Zhu, C.; Shen, H.Z.; Li, W.; Wang, B.; et al. Emissions of PAHs from indoor crop residue burning in a typical rural stove: Emission factors, size distributions, and gas-particle partitioning. *Environ. Sci. Tech.* **2011**, *45*, 1206–1212. [CrossRef]
3. Gomes, J.F.P.; Bordado, J.C.M.; Albuquerque, P.C.S. On the assessment of exposure to airborne ultrafine particles in urban environments. *J. Toxicol. Environ. Health* **2012**, *75*, 1316–1329. [CrossRef]
4. Semple, S.; Garden, C.; Coggins, M.; Galea, K.S.; Whelan, P.; Cowie, H. Contribution of solid fuel, gas combustion, or tobacco smoke to indoor air pollutant concentrations in Irish and Scottish homes. *Indoor Air* **2012**, *22*, 212–223. [CrossRef]
5. WHO. Household fuel combustion. In *WHO Indoor Air Quality Guidelines*; World Health Organization: Geneva, Switzerland, 2014.
6. Zhang, J.; Smith, K.R. Indoor air pollution from household fuel combustion in China: A review. In Proceedings of the 10th International Conference on Indoor Air Quality and Climate Indoor Air Quality and Climate, Beijing, China, 4–9 September 2005; pp. 65–83.
7. Wang, Z.J.; Xie, D.D.; Tang, R. Indoor air pollutants and their correlation at rural houses in severe cold region in winter. *J. Harbin Inst. Tech.* **2014**, *46*, 60–64. (In Chinese)
8. Zhao, B.; Zhang, Y.; Li, X.T.; Yang, X.D.; Huang, D.T. Comparison of indoor aerosol particle concentration and deposition in different ventilated rooms by numerical method. *Build. Environ.* **2004**, *39*, 1–8. [CrossRef]
9. Tian, Z.F.; Tu, J.Y.; Yeoh, G.H.; Yuen, R.K.K. On the numerical study of contaminant particle concentration in indoor airflow. *Build. Environ.* **2006**, *41*, 1504–1514. [CrossRef]
10. Kong, M.; Zhang, J.S.; Wang, J.J. Air and air contaminant flows in office cubicles with and without personal ventilation: A CFD modeling and simulation study. *Build. Simul.* **2015**, *8*, 381–392. [CrossRef]
11. Liu, Y.; Li, H.X.; Feng, G.H. Simulation of inhalable aerosol particle distribution generated from cooking by Eulerian approach with RNG *k*-epsilon turbulence model and pollution exposure in a residential kitchen space. *Build. Simul.* **2017**, *10*, 135–144. [CrossRef]
12. Zhang, Y.; Zhao, B. Simulation and health risk assessment of residential particle pollution by coal combustion in China. *Build. Environ.* **2007**, *42*, 614–622. [CrossRef]
13. Thatcher, T.L.; Layton, D.W. Deposition, resuspension, and penetration of particles within a residence. *Atmos. Environ.* **1995**, *29*, 1487–1497. [CrossRef]
14. Li, Y.G.; Chen, Z.D. A balance-point method for assessing the effect of natural ventilation on indoor particle concentrations. *Atmos. Environ.* **2003**, *37*, 4277–4285. [CrossRef]
15. Xie, W.; Fan, Y.S.; Wang, H.; Zhang, X.; Tian, G.J.; Si, P.F. Pre-valuation of indoor $PM_{2.5}$ concentration based on lumped parameter model. *China Environ. Sci.* **2020**, *40*, 539–545. (In Chinese)

16. Stewart, J.; Ren, Z.G. COwZ-A subzonal indoor airflow, temperature and contaminant dispersion model. *Build. Environ.* **2006**, *41*, 1631–1648. [CrossRef]
17. Dimitroulopoulou, C.; Ashmore, M.R.; Hill, M.T.R.; Byrne, M.A.; Kinnersley, R. INDAIR: A probabilistic model of indoor air pollution in UK homes. *Atmos. Environ.* **2006**, *40*, 6362–6379. [CrossRef]
18. Shen, L.; Deng, Q.H. Implementation, and control of asymmetric thermal environment in two-dimensional rectangular enclosure. *J. Cent. South. Univ. Tech.* **2005**, *12*, 262–267. [CrossRef]
19. Zhang, Z.; Chen, Q. Comparison of the Eulerian and Lagrangian methods for predicting particle transport in enclosed spaces. *Atmos. Environ.* **2007**, *41*, 5236–5248. [CrossRef]
20. Fabian, P.; Adamkiewicz, G.; Levy, J.I. Simulating indoor concentrations of NO_2 and $PM_{2.5}$ in multifamily housing for use in health-based intervention modeling. *Indoor Air* **2012**, *22*, 12–23. [CrossRef]
21. McGrath, J.A.; Byrne, M.A.; Ashmore, M.R.; Terry, A.C.; Dimitroulopoulou, C. Development of a probabilistic multi-zone multi-source computational model and demonstration of its applications in predicting PM concentrations indoors. *Sci. Total Environ.* **2014**, *490*, 798–806. [CrossRef]
22. Lee, B.H.; Yee, S.W.; Kang, D.H.; Yeo, M.S.; Kim, K.W. Multi-zone simulation of outdoor particle penetration and transport in a multi-story building. *Build. Simul.* **2017**, *10*, 525–534. [CrossRef]
23. Ferro, A.R.; Klepeis, N.E.; Ott, W.R.; Nazaroff, W.W.; Hildemann, L.M.; Switzer, P. Effect of interior door position on room-to-room differences in residential pollutant concentrations after short-term releases. *Atmos. Environ.* **2009**, *43*, 706–714. [CrossRef]
24. McGrath, J.A.; Byrne, M.A.; Ashmore, M.R.; Terry, A.C.; Dimitroulopoulou, C. A simulation study of the changes in $PM_{2.5}$ concentrations due to interzonal airflow variations caused by internal door opening patterns. *Atmos. Environ.* **2014**, *87*, 183–188. [CrossRef]
25. Zhao, J.Y. *Research on the Low-Cost Energy-Efficient Optimization of Rural House in Central Liaoning to Meet Indoor Thermal Environment Requirements*; Dalian University of Technology: Dalian, China, 2021. (In Chinese)
26. Zhuang, Z.; Li, Y.G.; Chen, B.; Guo, J.Y. Chinese kang as a domestic heating system in rural northern China—A review. *Energy Build.* **2009**, *41*, 111–119. [CrossRef]
27. Fang, X.M. *Building Environment Testing Technology*; China Construction Industry Press: Beijing, China, 2002. (In Chinese)
28. *GB 3095–2012*; Ministry of Ecology and Environment of the People's Republic of China, Ambient Air Quality Standards. China Environmental Science Press: Beijing, China, 2012. (In Chinese)
29. Ferro, A.R.; Kopperud, R.J.; Hildemann, L.M. Source strengths for indoor human activities that resuspend particulate matter. *Environ. Sci. Tech.* **2004**, *38*, 1759–1764. [CrossRef] [PubMed]
30. Lorenzetti, D.M. Computational aspects of nodal multizone airflow systems. *Build. Environ.* **2002**, *37*, 1083–1090. [CrossRef]
31. *GB/T 18883–2002*; Ministry of Ecology and Environment of the People's Republic of China, Indoor Air Quality Standards. Standards Press of China: Beijing, China, 2002. (In Chinese)
32. Byrne, M.A.; Goddard, A.J.H.; Lange, C.; Roed, J. Stable tracer aerosol deposition measurements in a test chamber. *J. Aerosol. Sci.* **1995**, *26*, 645–653. [CrossRef]
33. Fogh, C.L.; Byrne, M.A.; Roed, J.; Goddard, A.J.H. Size specific indoor aerosol deposition measurements and derived I/O concentrations ratios. *Atmos. Environ.* **1997**, *31*, 2193–2203. [CrossRef]
34. Thatcher, T.L.; Lunden, M.M.; Revzan, K.L.; Sextro, R.G.; Brown, N.J. A concentration rebound method for measuring particle penetration and deposition in the indoor environment. *Aerosol. Sci. Tech.* **2003**, *37*, 847–864. [CrossRef]
35. Mleczkowska, A.; Strojecki, M.; Bratasz, Ł.; Kozłowski, R. Particle penetration and deposition inside historical churches. *Build. Environ.* **2016**, *95*, 291–298. [CrossRef]
36. Liu, D.L.; Nazaroff, W.W. Particle penetration through building cracks. *Aerosol Sci. Technol.* **2003**, *37*, 565–573. [CrossRef]
37. Borrego, C.; Tchepel, O.; Costa, A.M.; Martins, H.; Ferreira, J.; Miranda, A.I. Traffic-related particulate air pollution exposure in urban areas. *Atmos. Environ.* **2006**, *37*, 7205–7214. [CrossRef]
38. McGrath, J.A.; Sheahan, J.N.; Dimitroulopoulou, C.; Ashmore, M.R.; Terry, A.C.; Byrne, M.A. PM exposure variations due to different time activity profile simulations within a single dwelling. *Build. Environ.* **2017**, *116*, 55–63. [CrossRef]
39. Kousa, A.; Monn, C.; Rotko, T.; Alm, S.; Oglesby, L.; Jantunen, M.J. Personal exposures to NO_2 in the EXPOLIS-study: Relation to residential indoor, outdoor and workplace concentrations in Basel, Helsinki and Prague. *Atmos. Environ.* **2001**, *35*, 3405–3412. [CrossRef]
40. Jiang, R.T.; Viviana, A.B.; Cheng, K.C.; Klepeis, N.E.; Ott, W.R.; Hildemann, L.M. Determination of response of real-time SidePak AM510 monitor to secondhand smoke, other common indoor aerosols, and outdoor aerosol. *J. Environ. Monit.* **2011**, *13*, 1695–1702. [CrossRef] [PubMed]
41. Aquilina, N.J.; Camilleri, S.F. Impact of daily household activities on indoor $PM_{2.5}$ and black carbon concentrations in Malta. *Build. Environ.* **2022**, *207*, 1–9. [CrossRef]
42. Gao, J.; Cao, C.S.; Xiao, Q.F.; Xu, B.; Zhou, X.; Zhang, X. Determination of dynamic intake fraction of cooking-generated particles in the kitchen. *Build. Environ.* **2013**, *65*, 146–153.
43. Bordado, J.C.; Gomes, J.F.; Albuquerque, P.C. Exposure to airborne ultrafine particles from cooking in Portuguese homes. *J. Air Waste Manag. Association.* **2012**, *62*, 1116–1126. [CrossRef] [PubMed]
44. He, C.R.; Morawska, L.D.; Hitchins, J.; Gilbert, D. Contribution from indoor sources to particle number and mass concentrations in residential houses. *Atmos. Environ.* **2004**, *38*, 3405–3415. [CrossRef]

45. Buonanno, G.; Morawska, L.; Stabile, L. Particle emission factors during cooking activities. *Atmos. Environ.* **2009**, *43*, 3235–3242. [CrossRef]
46. Dacunto, P.J.; Cheng, K.C.; Viviana, A.B.; Jiang, R.T.; Klepeis, N.E.; Repace, J.L.; Ott, W.R.; Hildemann, L.M. Real-time particle monitor calibration factors and PM2.5 emission factors for multiple indoor sources. *Environ. Sci. Processes Impacts.* **2013**, *15*, 1511–1519. [CrossRef]
47. Wangchuk, T.; He, C.; Knibbs, L.D.; Mazaheri, M.; Morawska, L. A pilot study of traditional indoor biomass cooking and heating in rural Bhutan: Gas and particle concentrations and emission rates. *Indoor Air* **2017**, *27*, 160–168. [CrossRef]
48. Vicente, E.D.; Vicente, A.M.; Evtyugina, M.; Oduber, F.I.; Amato, F.; Querol, X.; Alves, C. Impact of wood combustion on indoor air quality. *Sci. Total Environ.* **2020**, *705*, 1–17. [CrossRef] [PubMed]